Inorganic Chemistry
Article
Cite This: Inorg. Chem. 2018, 57, 2603−2608
pubs.acs.org/IC

Relevance of Orbital Interactions and Pauli Repulsion in the Metal−Metal Bond of Coinage Metals

Maria B. Brands,[†] Jörn Nitsch,*[,†] and Célia Fonseca Guerra*[,†,‡]

[†]Department of Theoretical Chemistry and Amsterdam Center for Multiscale Modeling, Vrije Universiteit Amsterdam, De Boelelaan 1083, 1081 HV Amsterdam, The Netherlands

[‡]Leiden Institute of Chemistry, Gorlaeus Laboratories, Leiden University, P.O. Box 9502, 2300 RA Leiden, The Netherlands

Supporting Information

ABSTRACT: The importance of relativity and dispersion in metallophilicity has been discussed in numerous studies. The existence of hybridization in the bonding between closed shell $d^{10}-d^{10}$ metal atoms has also been speculated, but the presence of attractive MO interaction in the metal−metal bond is still a matter of an ongoing debate. In this comparative study, a quantitative molecular orbital analysis and energy decomposition is carried out on the metallophilic interaction in atomic dimers ($M^+\cdots M^+$) and molecular perpendicular $[H_3P-M-X]_2$ (where M = Cu, Ag, and Au; X = F, Cl, Br, and I). Our computational studies prove that besides the commonly accepted dispersive interactions, orbital interactions and Pauli repulsion also play a crucial role in the strength and length of the metal−metal bond. Although for $M^+\cdots M^+$ the orbital interaction is larger than the Pauli repulsion, leading to a net attractive MO interaction, the bonding mechanism in perpendicular $[H_3P-M-X]$ dimers is different due to the larger separation between the donor and acceptor orbitals. Thus, Pauli repulsion is much larger, and two-orbital, four-electron repulsion is dominant.

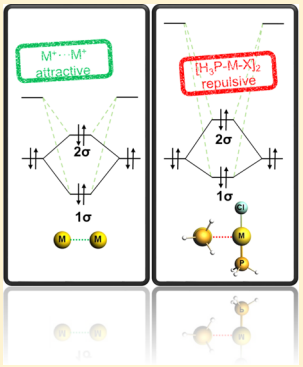

INTRODUCTION

Closed-shell $d^{10}-d^{10}$ interactions are an interesting research target both from an experimental as well as from a theoretical perspective.[1] From a practical point of view, these interactions can be used for the design of supramolecular (di-, oligo-, or polymeric) structures.[1j] Furthermore, these structures show very interesting luminescence properties, including mechanochromic or vaporchromic behavior[2a−l] and are discussed as important viable intermediate in gold-catalyzed hydroarylation reactions.[2m] In addition, complexes displaying metallophilic interactions are also considered as potential antitumor agents.[3] The strength of aurophilic interactions has been determined experimentally in some cases and is comparable to moderate H-bonds (7−12 kcal/mol).[4] However, for an effective tuning of such interactions, it is crucial to understand the bonding mechanism behind $d^{10}-d^{10}$ metallophilic interactions. This mechanism is still a subject of a long-standing debate and has proven quite a challenge for quantum chemistry. There is a broad consensus that relativity and dispersion in metallophilicity play an important role.[1] From a molecular orbital (MO) perspective, attractive interaction is not expected *a priori* in closed-shell atoms (consider He_2 or a hydride dimer as examples, where two-orbital, four-electron repulsion are dominant). However, pioneering work conducted by Hoffmann et al. in 1978, concluded from extended Hückel theory (EHT) that hybridization of empty $(n + 1)$s and filled nd_{z^2} orbitals is present and accounts for a covalent metal−metal bond in systems such as dicationic $Cu^+\cdots Cu^+$ or in neutral $[Au_2(S_2PH_2)_2]$.[5] Since then different views have been presented. While others including Schmidbaur[6] and Mingos[7] also mentioned the importance of 5d and 6s hybridization in the bonding of Au clusters, Pyykkö concluded that there is no hybridization present.[8] He showed that electron correlation strengthened by relativity is of great importance (i.e., that dispersive effects are only responsible for the attractive interaction in coinage metal dimers). In turn, Schwarz[9] could find for the perpendicular $[H_3P-Au-Cl]_2$ (Figure 1; structure B, M = Au, X = Cl) an orbital interaction energy of −21 kcal/mol, which he also attributed to orbital mixing. However, the conclusions presented by Schwarz are derived from a simple local $X\alpha$ exchange potential (S-LDF) DFT calculation and could be attributed to the fortuitous cancellation of errors.

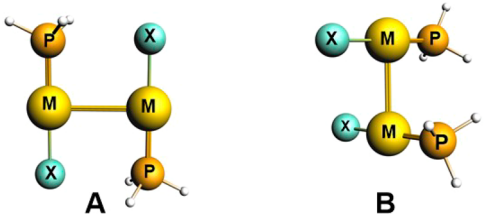

Figure 1. Head-to-tail (**A**) and perpendicular (**B**) $[H_3P-M-X]_2$ with M = Cu, Ag, and Au; X = F, Cl, Br, and I (X−M−M−X and P−M−M−P dihedral angles are constrained to 180.0° (**A**) and 90.0° (**B**). For full details, see the Supporting Information.

Received: November 29, 2017
Published: February 12, 2018

DOI: 10.1021/acs.inorgchem.7b02994
Inorg. Chem. 2018, 57, 2603−2608

At this point, no consensus is reached on the bonding mechanism in metallophilic interactions. Thus, we have analyzed the bonding mechanism in the framework of Kohn–Sham molecular orbital theory and would like to emphasize a neglected aspect of this discussion: the importance of Pauli repulsion and orbital interaction in metallophilicity.

THEORETICAL METHODS

Herein, we present an energy decomposition analysis (EDA)[10] of the metal–metal bond in perpendicular dimers such as $[H_3P–M–X]_2$ (see Figure 1, (**B**), M = Cu, Ag, and Au; X = F, Cl, Br, and I) and compared these systems with simple metal dimers ($M^+\cdots M^+$). De Proft used a similar approach for analyzing the interaction in $[NHC–M–Cl]_2$ (where NHC is an *N*-heterocyclic carbene).[11] In contrast to our studies, a head-to-tail arrangement (see Figure 1; structure type **A**) of these dimers was used instead, which includes additional ligand–ligand interactions besides metallophilicity (*vide infra*).

We performed a benchmark of our dispersion-corrected DFT methods (see Tables S1–S3) and decided to use the ZORA-BLYP-D3(BJ)/TZ2P level of theory (MAE: 0.3–2.4 kcal/mol; Supporting Information). The dimerization energy (ΔE_{dim}) of forming $[H_3P–M–X]_2$ from their respective monomers can be decomposed in the following terms:

$$\Delta E_{dim} = \Delta E_{int} + \Delta E_{prep} \quad (1)$$

$$\Delta E_{int} = \Delta E_{Pauli} + \Delta V_{elstat} + \Delta E_{disp} + \Delta E_{oi} \quad (2)$$

ΔE_{prep} is the preparation or strain energy of the two (deformed) fragments ($[H_3P–M–X]^{‡}$) and ΔE_{int} is the interaction energy between these deformed reactants (eq 1). The latter can be further analyzed in the conceptual framework provided by the Kohn–Sham molecular orbital model and decomposed into physically meaningful terms (eq 2). The EDA quantifies the Pauli-repulsive orbital interactions (ΔE_{Pauli}) between same-spin electrons, the electrostatic interaction (ΔV_{elstat}), interaction due to dispersion forces (ΔE_{disp}), and orbital interactions (ΔE_{oi}) that emerge from charge transfer (interaction between occupied orbitals on one fragment with unoccupied orbitals on the other fragment, including donor–acceptor interactions) and polarization (empty–occupied orbital mixing on one fragment due to the presence of the other fragment).

RESULTS AND DISCUSSION

The equilibrium bond distances *r* of structures **A** (head-to-tail) and **B** (perpendicular) for M = Cu, Ag, and Au and X = F, Cl, Br, and I can be found in Table S4. For all cases, the head-to-tail dimers are more stable with respect to dissociation than the structures of the perpendicular arrangement. Thus, structures **A** have more attractive dimerization energies (**A**: between −16 and −24 kcal/mol; **B**: between −8 and −15). The difference in dimer stability between **A** and **B** becomes less pronounced the larger the halogen atom X becomes (*F* < Cl < Br < I), which is accompanied in structure **A** by an increase of the r_{MM} distance (as an example, $[H_3P–Cu–F]_2$: r_{MM} = 2.76 Å; $[H_3P–Cu–I]_2$: r_{MM} = 3.69 Å). This increase in the equilibrium metal–metal distance is not found for the perpendicular dimers ($[H_3P–Cu–F]_2$: r_{MM} = 2.71 Å; $[H_3P–Cu–I]_2$: r_{MM} = 2.69 Å). It is clear that for the head-to-tail arrangement additional ligand–ligand interactions lead to a stabilization of the dimer. Thus, we will focus in the following on structure **B**, where ligand–ligand interactions are minimized.

In order to examine the metal–metal bond exclusively, we will first consider the MO diagram and energy decomposition of the bare metal dimers ($M^+\cdots M^+$), in the absence of any ligand. We choose a metal–metal distance (r_{MM}), which is equal to the equilibrium distance in perpendicular $[H_3P–M–Cl]$ dimers (Cu: 2.71 Å; Ag: 2.97 Å; Au: 3.15 Å). The MO diagram for the $M^+\cdots M^+$ interaction is displayed in Figure 2.

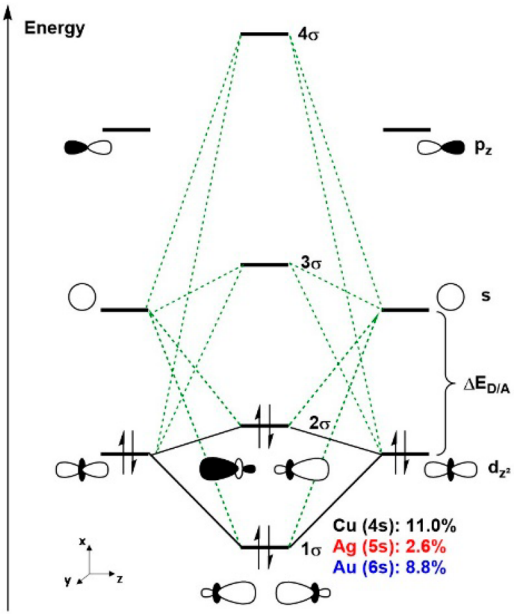

Figure 2. Schematic MO diagram for $M^+\cdots M^+$. s-Orbital contribution [in %] to 1σ is also shown (compare text). The green dotted lines indicate the mixing in of empty s and filled d_{z^2} in the bonding and antibonding MOs. Distance (r_{MM}) is shown in Table 1.

It is apparent that the 1σ orbital is the bonding and 2σ is the antibonding combination of the metal–metal interaction. Hence, our results derived from KS-MO theory are in a qualitative agreement with the extended Hückel theory (EHT) picture from Hoffmann.[5a]

Figure 2 and Table S5 show the percentages of the relevant orbitals derived from a gross orbital population analysis. Mixing in of the empty (*n* + 1)s orbital leads to a stabilization of the 1σ and to a smaller extend of the 2σ. The largest (*n* + 1)s orbital admixture to 1σ is found for Cu (11.0%), followed by Au (8.8%) and Ag (2.6%). The admixture of $(n + 1)p_z$ is in general much smaller and is up to 3% (Cu) and smaller for gold (2%) and silver (1%) (see Table S5).

The EDA results are shown in Table 1 and reveal an entirely positive (repulsive) interaction energy (ΔE_{int}), where the least

Table 1. EDA of $M(1)^+\cdots M(2)^+$[a]

$M^+\cdots M^+$	r_{MM} [Å]	ΔE_{Pauli}	ΔV_{elstat}	ΔE_{disp}	ΔE_{oi}	ΔE_{int}
$Cu^+\cdots Cu^+$	2.71	3.6	119.1	−2.3	−21.8	98.7
$Ag^+\cdots Ag^+$	2.97	3.8	109.2	−2.5	−12.3	98.2
$Au^+\cdots Au^+$	3.15	4.0	102.6	−2.5	−19.2	84.9

[a]All values are in kcal/mol. r_{MM} is equal to the equilibrium distance in $[H_3P–M–Cl]_2$.

repulsive ΔE_{int} is found for Au (84.9 kcal/mol) and being almost equal for Cu and Ag (98.7 and 98.2 kcal/mol). This repulsive interaction is mainly due to the (expected) large electrostatic repulsion of two cationic metal ions experiencing each other (ΔV_{elstat}: Au: 102.6 kcal/mol; Ag: 109.2 kcal/mol; Cu: 119.1 kcal/mol). The difference in ΔV_{elstat} can be explained by the difference in r_{MM} (Cu: 2.71 Å, Ag: 2.97 Å and Au: 3.01 Å). However, in accordance with the finding of Hoffmann and

DOI: 10.1021/acs.inorgchem.7b02994
Inorg. Chem. 2018, 57, 2603–2608

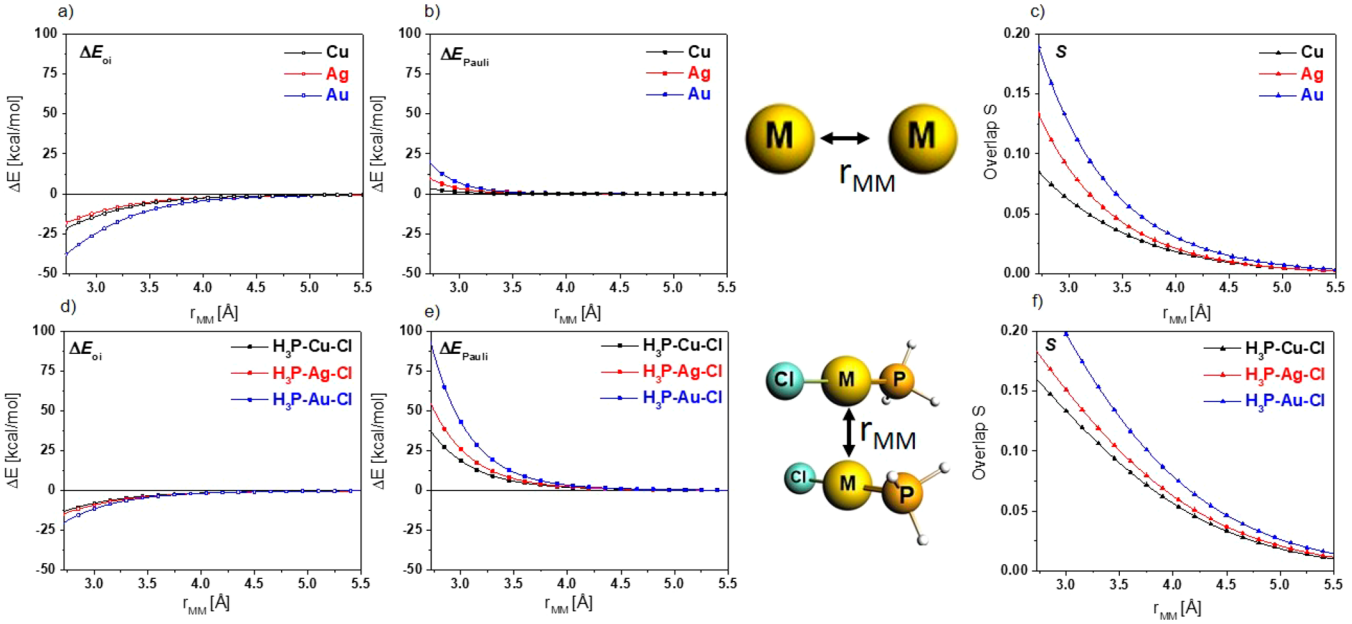

Figure 3. Orbital interaction (ΔE_{oi}), Pauli repulsion (ΔE_{Pauli}), and orbital overlap S of the five highest occupied FMOs of $M^+\cdots M^+$ (a–c) and $[H_3P-M-Cl]_2$ (d–f) at different distances: Cu (black), Ag (red), and Au (blue); X–M–M–X and L–M–M–L dihedral angle are constrained to 90.0°. For full details, see the Supporting Information.

in contrast to Pyykkö's conclusion, an attractive orbital interaction (ΔE_{oi}) is found (Cu: −21.8 kcal/mol; Ag: −12.2 kcal/mol; Au: −19.2 kcal/mol).

The trend in ΔE_{oi} can traced back to the contribution of metal $(n + 1)$s to the 1σ, which is related to the energy gap ($\Delta E_{D/A}$) between the n d_{z^2} (donor) and $(n + 1)$s (acceptor) orbital (Cu: 1.62 eV, Ag: 4.13 eV and Au: 1.97 eV). The small energy gap ($\Delta E_{D/A}$) for $Au^+\cdots Au^+$ is a consequence of the strong relativistic effects present for this metal, which causes a destabilization of the metal 5d and a stabilization 6s orbital.[12] Pauli repulsion (ΔE_{Pauli}), which is caused by antibonding orbital overlap (i.e., the 2σ MO and other filled d-orbitals) is much smaller (3.6–4.0 kcal/mol), making the closed shell interaction shown in Figure 2 *net attractive*. Thus, for the bare metal dimers, the closed shell d^{10}–d^{10} two-orbital, four-electron repulsion is weak, due to strong mixing in of the metal s orbital and the relative small antibonding orbital overlap (Cu: 8.5×10^{-2}; Ag: 9.1×10^{-2}; Au: 10.0×10^{-2}). Obviously, the energy terms of the EDA and the overlap S are functions of the metal–metal distance (r_{MM}), thus we have examined the different EDA terms for a range of metal–metal distances (see Figure 3a and 3b for ΔE_{oi} and ΔE_{Pauli}; Figure S2 for the full EDA).

However, the relative importance of each energy term remains unchanged (i.e., a strong electrostatic repulsion, large orbital interaction, and small Pauli repulsion). If the interaction energy is compared at the same metal–metal distance, then the most stabilizing ΔE_{oi} curve is found for Au followed by the almost identical curves for Cu and Ag (Figure 3a). In addition to the relative small value for $\Delta E_{D/A}$ the orbital overlap S for Au is larger than for Cu. Furthermore, Pauli repulsion plays a minor role and is smallest for Cu, followed by Ag and then by Au (Figure 3b), due to the smallest orbital overlap for copper (Cu < Ag < Au; Figure 3c). Succinctly, apart from the expected large electrostatic repulsion, orbital interaction is an important term in determining the metallophilic interaction of closed shell $M^+\cdots M^+$ systems and is mainly caused by mixing in (or hybridization) of $(n + 1)$s acceptor orbitals.

We will now consider the more realistic dicoordinated perpendicular model structures (Figure 1; structure **B**). A simplified MO for $[H_3P-Au-Cl]_2$ is shown in Figure 4 (see

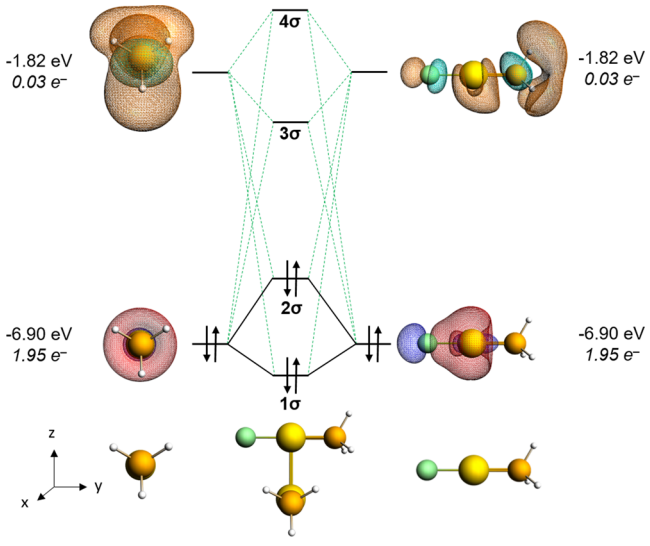

Figure 4. MO diagram for $[H_3P-Au-Cl]_2$. The black lines indicate the formation of bonding 1σ and antibonding combinations 2σ. The green dotted lines indicate the mixing in of empty and filled FMOs in the bonding and antibonding MOs. The isovalue is 0.03 e^-/a_0^3.

the Supporting Information for other structures). It is apparent from these plots that the mixing in of acceptor fragment molecular orbital(s) (FMO) leads to a stabilization of the 1σ and the 2σ. With respect to the metal–metal interaction, 1σ is bonding, whereas 2σ is antibonding, which is qualitatively equivalent to the situation in Figure 2, but the stabilization of these orbitals is now smaller, and the acceptor orbital is to a large extend a ligand orbital. Thus, this situation will lead, in

DOI: 10.1021/acs.inorgchem.7b02994
Inorg. Chem. 2018, 57, 2603–2608

Table 2. Results of the EDA for the Perpendicular $[H_3P{-}M{-}X]$ Dimers[a]

X	M	r_{MM} [Å]	ΔE_{Pauli}	ΔV_{elstat}	ΔE_{disp}	ΔE_{oi}	ΔE_{int}	ΔE_{dim}	occupancy of donor orbital[b]
	Cu	2.71	31.4	−22.0	−8.4	−11.2	−10.2	−9.9	1.93
F	Ag	3.00	22.7	−16.1	−9.1	−7.7	−10.2	−10.0	1.95
	Au	3.18	24.1	−16.6	−8.2	−7.3	−8.0	−7.9	1.96
	Cu	2.71	38.2	−25.7	−11.7	−13.3	−12.5	−12.1	1.93
Cl	Ag	2.97	28.4	−19.4	−10.8	−9.6	−11.4	−11.1	1.95
	Au	3.15	29.0	−19.4	−10.8	−8.6	−9.9	−9.7	1.95
	Cu	2.70	43.1	−28.9	−13.1	−14.9	−13.8	−13.4	1.93
Br	Ag	2.95	31.7	−21.7	−12.0	−10.6	−12.5	−12.2	1.95
	Au	3.13	32.1	−21.5	−12.0	−9.5	−10.9	−10.7	1.95
	Cu	2.69	50.0	−33.4	−15.2	−16.9	−15.6	−15.1	1.93
I	Ag	2.95	36.6	−25.0	−13.8	−12.0	−14.2	−13.8	1.95
	Au	3.11	36.8	−24.7	−12.3	−10.6	−10.8	−10.6	1.96

[a]All values are in kcal/mol. The equilibrium distances r_{MM} are also shown. [b]The initial occupancy of donor orbital D(1) or D(2) (see also Figure 5).

contrast to Figure 2, to a *net repulsive* MO interaction (*vide infra*).

Table 2 shows the dimerization energies (ΔE_{dim}) and the results of the EDA for various perpendicular $[H_3P{-}M{-}X]$ dimers at their equilibrium distances. In all cases, $[H_3P{-}Cu{-}X]_2$ has the most attractive (i.e., most negative) dimerization energies (−10 to −15 kcal/mol), followed by $[H_3P{-}Ag{-}X]_2$ (−10 to −14 kcal/mol) and then by $[H_3P{-}Au{-}X]_2$ (−8 to −11 kcal/mol), except for X = F, where ΔE_{dim} is almost equal for Ag and Cu. The most attractive dimerization energy is found for $[H_3P{-}Cu{-}I]_2$ (−15 kcal/mol), while the least attractive is found for $[H_3P{-}Au{-}F]_2$ (−8 kcal/mol). The dimerization energy (ΔE_{dim}) and interaction energy (ΔE_{int}) do not differ much; the preparation or strain energy (ΔE_{prep} in eq 1) ranges for all $[H_3P{-}M{-}X]_2$ systems between 0.2 and 0.4 kcal/mol. Thus, the dimerization does not lead to a large geometric change or deformation in the linear $[H_3P{-}M{-}X]$ monomers. The most attractive terms for all dimers are the electrostatic interactions. While ΔV_{elstat} for equal halogens (X) are similar for all $[H_3P{-}Ag{-}X]_2$ and $[H_3P{-}Au{-}X]_2$, ranging from −16 to −25 kcal/mol (from F to I), these interactions differ significantly for $[H_3P{-}Cu{-}X]$ dimers by an absolute value of about 6−8 kcal/mol (i.e., the electrostatic interactions are more attractive for Cu than for Ag and Au). This is due a larger electronic charge density overlap for $[H_3P{-}Cu{-}X]_2$ because of the shorter equilibrium distances for these structures (Figures S3−S6).[10b] A similar trend (opposite in sign) is found for the Pauli repulsion, where the values for Cu range between 31 and 50 kcal/mol, whereas for Ag/Au they are between 23 and 37 kcal/mol. In contrast to the bare metal dimers, the Pauli repulsion is for all structures the most dominant factor (largest absolute values) of determining the dimerization energy. Similar to the bare metal dimers, we found a non-neglectable orbital interaction energy (ΔE_{oi}). The most attractive orbital interaction is found for Cu (−12 to −17 kcal/mol), followed by Ag (−8 to −12 kcal/mol), and then closely followed by Au (−7 to −11 kcal/mol).

In general, ΔE_{oi} in $[H_3P{-}M{-}X]_2$ can either be caused by polarization (P) (i.e., mixing in of virtual orbitals on one fragment due to the presence of the other fragment; Figure 5, vertical arrows) or by charge transfer from one fragment to the unoccupied orbitals of the other (donor−acceptor interaction; Figure 5, diagonal arrows). We performed calculations where we deleted the virtual orbitals of one monomer (A(2)*, in Figure 5 right). After removing these orbitals, the donor orbital D(1) can no longer transfer electrons via D-A interactions to A(2)*. However, the vertical polarization D(1) → A(1)* can still occur. We carefully examined the gross electron population of the relevant frontier orbitals. As seen in Figure 5, for $[H_3P{-}Au{-}Cl]_2$ the population of D(1) changes from 1.95 to 2.00 when removing the virtual orbitals A(2)*. We found this behavior for all $[H_3P{-}M{-}X]$ dimers (see last column of Tables 2 and S6); therefore, we conclude that polarization plays only a minor role in these systems. We found, however, that polarization becomes more important for $M^+{\cdots}M^+$ (see Table S7).

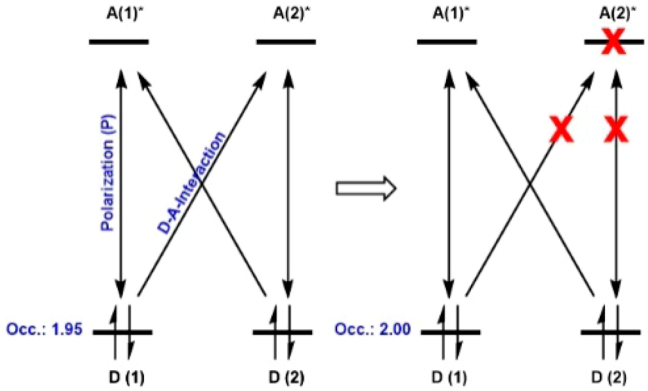

Figure 5. Schematic picture of donor−acceptor (D-A) interactions (e.g., D(1) → A(2)*) and polarization (P; e.g., D(1) → A(1)*). Change in occupation in $[H_3P{-}Au{-}Cl]_2$ is shown if virtual orbitals A(2)* of fragment 2 (i.e., of one $[H_3P{-}Au{-}Cl]$ monomer) are removed.

In contrast to the bonding mechanism found for bare metals dimers, the Pauli repulsion compensates for the orbital interactions by 13−33 kcal/mol for $[H_3P{-}M{-}X]_2$. This indicates inherently that occupied antibonding orbital combinations compensate the occupied bonding (i.e., two-orbital, four-electrons repulsion is dominant in Figure 4). This finding agrees with Pyykkö's conclusion regarding the overall absence of MO interactions for $[H_3P{-}M{-}X]_2$ and can be derived from a series of EDA at different metal−metal -distances as well (see Figures 3d−f and S2−S5). Nevertheless, without the ΔE_{oi} term, the dimerization energies of $[H_3P{-}M{-}X]_2$ would be largely reduced and in some cases, turn out positive (see ΔE_{dim} and ΔE_{oi} in Table 2), meaning that the monomers would repel each other.

The 1σ orbital consists of donor and acceptor FMO(s), where the main contributions to the donor orbitals come from

DOI: 10.1021/acs.inorgchem.7b02994
Inorg. Chem. 2018, 57, 2603−2608

the metal *n*d orbitals and where the acceptor orbitals consist mainly of ligand σ^* P−H orbitals and the metal $(n + 1)$s and $(n + 1)$p orbitals, indicating the influence of the ligand orbitals on metallophilic interactions of perpendicular dimers. In the equilibrium structures, there is a larger overlap with the acceptor orbitals for the 3d metal (Cu) than those for for 4d (Ag) and 5d (Au), and $\Delta E_{D/A}$ is larger for Ag than those for Au and Cu. Note that in the $[H_3P{-}M{-}X]$ dimers the $\Delta E_{D/A}$ gap between donor and acceptor is much higher (4.20−6.13 eV) than those in the bare metals (1.62−4.13 eV), which prevents a comparable mixing in of acceptor orbitals in these systems.

CONCLUSION

The MO analysis of $M^+\cdots M^+$ is in a qualitative agreement with the hybridization picture introduced by Hoffmann[4a] (i.e., there is covalent attractive contribution to the metal−metal interaction). However, it is important to mention that if ligands are present, like in $[H_3P{-}M{-}X]_2$, Pauli repulsion is much more important than ΔE_{oi} (compare Figure 3a,b with Figure 3d,e). In these cases, the electrostatic energy is the largest attractive interaction term. Still, attractive D−A interaction is present, but is overruled by two-orbital, four-electron repulsion. Nevertheless, mixing of acceptor orbitals into the 1σ leads to a stabilization of $[H_3P{-}M{-}X]_2$ systems, which would otherwise be nonbonding. Thus, an effective tuning of these interactions could be achieved if the acceptor orbitals are significantly stabilized. Studies which focus on the influence of the ligand acceptor orbital(s) are currently under progress.

ASSOCIATED CONTENT

Supporting Information

The following files are available free of charge. SI_Inorg_Chem.pdf . The Supporting Information is available free of charge on the ACS Publications website at DOI: 10.1021/acs.inorgchem.7b02994.

Details of the computational methods, benchmark study, equilibrium bond distances (r) and dimerization energies of the optimized head-to-tail and perpendicular $[H_3P{-}M{-}X]$ dimers, gross orbital population analysis of the $M^+\cdots M^+$ interaction, EDA of $M^+\cdots M^+$ and $[H_3P{-}M{-}X]_2$ at different distances, total SFO gross populations analysis of donor and acceptor orbitals in $M^+\cdots M^+$ and $[H_3P{-}M{-}X]_2$, major fragment molecular orbitals (FMOs) of the donor−acceptor interaction in $[H_3P{-}M{-}X]_2$, coordinates (XYZ) and constraints of all structures used in this study, including total bonding energies (TBE) and frequency analysis (PDF)

AUTHOR INFORMATION

Corresponding Authors

*E-mail: j.s.n.nitsch@vu.nl.
*E-mail: c.fonsecaguerra@vu.nl.

ORCID

Jörn Nitsch: 0000-0002-4005-2257
Célia Fonseca Guerra: 0000-0002-2973-5321

Notes

The authors declare no competing financial interest.

ACKNOWLEDGMENTS

J.N. thanks the DFG for a Postdoctoral Research Fellowship (NI 1737/1-1). C.F.G. thanks The Netherlands Organization for Scientific Research (NWO/CW) for financial support.

REFERENCES

(1) (a) Pyykkö, P. Strong Closed-Shell Interactions in Inorganic Chemistry. *Chem. Rev.* **1997**, *97*, 597−636. (b) Pyykkö, P. Theoretical chemistry of gold. *Angew. Chem., Int. Ed.* **2004**, *43*, 4412−4456. (c) O'Grady, E.; Kaltsoyannis, N. Does metallophilicity increase or decrease down group 11? Computational investigations of $[Cl{-}M{-}PH_3]_2$ (M = Cu, Ag, Au, [111]). *Phys. Chem. Chem. Phys.* **2004**, *6*, 680−687. (d) Schmidbaur, H.; Cronje, S.; Djordjevic, B.; Schuster, O. Understanding gold chemistry through relativity. *Chem. Phys.* **2005**, *311*, 151−161. (e) Pyykkö, P. Theoretical chemistry of gold. III. *Chem. Soc. Rev.* **2008**, *37*, 1967−1997. (f) Schmidbaur, H.; Schier, A. A briefing on aurophilicity. *Chem. Soc. Rev.* **2008**, *37*, 1931−1951. (g) Pyykkö, P.; Xiong, X.-G.; Li, J. Aurophilic attractions between a closed-shell molecule and a gold cluster. *Faraday Discuss.* **2011**, *152*, 169−178. (h) Muñiz, J.; Wang, C.; Pyykkö, P. Aurophilicity: The Effect of the Neutral Ligand L on $[\{ClAuL\}_2]$ Systems. *Chem. - Eur. J.* **2011**, *17*, 368−377. (i) Sculfort, S.; Braunstein, P. Intramolecular d^{10}-d^{10} interactions in heterometallic clusters of the transition metals. *Chem. Soc. Rev.* **2011**, *40*, 2741−2760. (j) Schmidbaur, H.; Schier, A. Aurophilic interactions as a subject of current research: an up-date. *Chem. Soc. Rev.* **2012**, *41*, 370−412. (k) Hupf, E.; Kather, R.; Vogt, M.; Lork, E.; Mebs, S.; Beckmann, J. Dispersion in Metallophilic Hg···M Interactions (M = Cu, Ag, Au) within Coinage Metal Complexes of Bis(6-diphenylphosphinoacenaphth-5-yl)mercury. *Inorg. Chem.* **2016**, *55*, 11513−11521.

(2) (a) Che, C.-M.; Lai, S.-W. Structural and spectroscopic evidence for weak metal-metal interactions and metal-substrate exciplex formations in d^{10} metal complexes. *Coord. Chem. Rev.* **2005**, *249*, 1296−1309. (b) Phillips, D. L.; Che, C.-M.; Leung, K. H.; Mao, Z.; Tse, M.-C A comparative study on metal-metal interaction in binuclear two- and three-coordinated d^{10}-metal complexes. Spectroscopic investigation of M(I)-M(I) interaction in the $^1[d\sigma^*p\sigma]$ excited state of $[M_2(dcpm)_2]^{2+}$ (dcpm = bis(dicyclohexylphosphino)methane) (M = Au, Ag, Cu) and $[M_2(dmpm)_3]^{2+}$ (dmpm = bis-(dimethylphosphino)methane) (M = Au, Ag, Cu) complexes. *Coord. Chem. Rev.* **2005**, *249*, 1476−1490. (c) Chen, Z. N.; Zhao, N.; Fan, Y.; Ni, J. Luminescent groups 10 and 11 heteropolynuclear complexes based on thiolate or alkynyl ligands. *Coord. Chem. Rev.* **2009**, *253*, 1−20. (d) Ito, H.; Muromoto, M.; Kurenuma, S.; Ishizaka, S.; Kitamura, N.; Sato, H.; Seki, T. Mechanical stimulation and solid seeding trigger single-crystal-to-single-crystal molecular domino transformations. *Nat. Commun.* **2013**, *4*, 2009. (e) Vickery, J. C.; Olmstead, M. M.; Fung, E. Y.; Balch, A. L. Solvent-stimulated luminescence from the supramolecular aggregation of a trinuclear gold(I) complex that displays extensive intermolecular Au-Au interactions. *Angew. Chem., Int. Ed. Engl.* **1997**, *36*, 1179−1181. (f) Mansour, M. A.; Connick, W. B.; Lachicotte, R. J.; Gysling, H. J.; Eisenberg, R. Linear chain Au(I) dimer compounds as environmental sensors: A luminescent switch for the detection of volatile organic compounds. *J. Am. Chem. Soc.* **1998**, *120*, 1329−1330. (g) Seki, T.; Sakurada, K.; Muromoto, M.; Seki, S.; Ito, H. Detailed Investigation of the Structural, Thermal, and Electronic Properties of Gold Isocyanide Complexes with Mechano-Triggered Single-Crystal-to-Single-Crystal Phase Transitions. *Chem. - Eur. J.* **2016**, *22*, 1968−1978. (h) Nitsch, J.; Lacemon, F.; Lorbach, A.; Eichhorn, A.; Cisnetti, F.; Steffen, A. Cuprophilic interactions in highly luminescent dicopper(I)-NHC-picolyl complexes - fast phosphorescence or TADF? *Chem. Commun.* **2016**, *52*, 2932−2935. (i) El Sayed Moussa, M.; Evariste, S.; Wong, H. L.; Le Bras, L.; Roiland, C.; Le Polles, L.; Le Guennic, B.; Costuas, K.; Yam, V. W.-W.; Lescop, C. A solid state highly emissive Cu(I) metallacycle: promotion of cuprophilic interactions at the excited states. *Chem. Commun.* **2016**, *52*, 11370−11373. (j) Lima, J. C.; Rodríguez, L. Applications of gold(I) alkynyl systems: a growing field to explore. *Chem. Soc. Rev.*

DOI: 10.1021/acs.inorgchem.7b02994
Inorg. Chem. 2018, 57, 2603−2608

2011, *40*, 5442−5456. (k) Che, C.-M.; Kwong, H.-L.; Yam, V. W.-W.; Cho, K.-C. Spectroscopic properties and redox chemistry of the phosphorescent excited state of $[Au_2(dppm)_2]^{2+}$ [dppm = bis-(diphenylphosphino)methane]. *J. Chem. Soc., Chem. Commun.* **1989**, 885−886. (l) Bestgen, S.; Gamer, M. T.; Lebedkin, S.; Kappes, M. M.; Roesky, P. W. Di- and trinuclear gold complexes of diphenylphosphinoethyl-functionalised imidazolium salts and their N-heterocyclic carbenes: synthesis and photophysical properties. *Chem. - Eur. J.* **2015**, *21*, 601−614. (m) Gagné, M. R.; Weber, D. In *Homogeneous Gold Catalysis*; Springer International Publishing: Cham, 2015; Vol. *357*, pp 167−212 (and references herein).

(3) (a) Barreiro, E.; Casas, J. S.; Couce, M. D.; Laguna, A.; López-de-Luzuriaga, J. M.; Monge, M.; Sánchez, A.; Sordo, J.; Varela, J. M.; López, E. M. V. A Dinuclear Gold(I)-Silver(I) Derivative of 2-Cyclopentylidene-2-sulfanylacetic Acid and Related Complexes: Synthesis, Crystal Structures, Properties and Antitumor Activity. *Eur. J. Inorg. Chem.* **2011**, *2011*, 1322−1332. (b) Barreiro, E.; Casas, J. S.; Couce, M. D.; Sánchez, A.; Sánchez-González, A.; Sordo, J.; Varela, J. M.; Vázquez López, E. M. Dinuclear triphenylphosphinegold(I) sulfanylcarboxylates: Synthesis, structure and cytotoxic activity against cancer cell lines. *J. Inorg. Biochem.* **2010**, *104*, 551−559.

(4) (a) Schmidbaur, H.; Dziwok, K.; Grohmann, A.; Müller, G. Further Evidence for Attractive Interactions between Gold(I) Centers in Binuclear Complexes. *Chem. Ber.* **1989**, *122*, 893−895. (b) Harwell, D. E.; Mortimer, M. D.; Knobler, C. B.; Anet, F. A. L.; Hawthorne, M. F. Auracarboranes with and without Au-Au interactions: An unusually strong aurophilic interaction. *J. Am. Chem. Soc.* **1996**, *118*, 2679−2685. (c) Deák, A.; Megyes, T.; Tárkányi, G.; Király, P.; Biczók, L.; Pálinkás, G.; Stang, P. J. Synthesis and solution- and solid-state characterization of gold(I) rings with short Au···Au interactions. Spontaneous resolution of a gold(I) complex. *J. Am. Chem. Soc.* **2006**, *128*, 12668−12670. (d) Arunan, E.; Desiraju, G. R.; Klein, R. A.; Sadlej, J.; Scheiner, S.; Alkorta, I.; Clary, D. C.; Crabtree, R. H.; Dannenberg, J. J.; Hobza, P.; Kjaergaard, H. G.; Legon, A. C.; Mennucci, B.; Nesbitt, D. J. Defining the hydrogen bond: An account. *Pure Appl. Chem.* **2011**, *83*, 1619−1636.

(5) (a) Mehrotra, P. K.; Hoffmann, R. Cu(I)-Cu(I) Interactions - Bonding Relationships in d^{10}-d^{10} Systems. *Inorg. Chem.* **1978**, *17*, 2187−2189. (b) Jiang, Y.; Alvarez, S.; Hoffmann, R. Binuclear and Polymeric Gold(I) Complexes. *Inorg. Chem.* **1985**, *24*, 749−757.

(6) Görling, A.; Rösch, N.; Ellis, D. E.; Schmidbaur, H. Electronic structure of main-group-element-centered octahedral gold clusters. *Inorg. Chem.* **1991**, *30*, 3986−3994.

(7) Evans, D. G.; Mingos, D. M. P. Molecular orbital analysis of the bonding in penta- and hepta-nuclear gold tertiary phosphine clusters. *J. Organomet. Chem.* **1985**, *295*, 389−400.

(8) (a) Pyykkö, P.; Zhao, Y. F. Ab initio Calculations on the $(ClAuPH_3)_2$ Dimer with Relativistic Pseudopotential - Is the Aurophilic Attraction a Correlation Effect? *Angew. Chem., Int. Ed. Engl.* **1991**, *30*, 604−605. (b) Li, J.; Pyykkö, P. Relativistic Pseudopotential Analysis of the Weak Au(I)···Au(I) Attraction. *Chem. Phys. Lett.* **1992**, *197*, 586−590. (c) Pyykkö, P.; Li, J.; Runeberg, N. Predicted Ligand Dependence of the Au(I)···Au(I) Attraction in $(XAuPH_3)_2$. *Chem. Phys. Lett.* **1994**, *218*, 133−138.

(9) Wang, S. G.; Schwarz, W. H. Quasi-relativistic density functional study of aurophilic interactions. *J. Am. Chem. Soc.* **2004**, *126*, 1266−1276.

(10) (a) Ziegler, T.; Rauk, A. On the calculation of bonding energies by the Hartree Fock Slater method. I. The transition state method. *Theor. Chim. Acta* **1977**, *46*, 1−10. (b) Bickelhaupt, F. M.; Baerends, E. J. Kohn-Sham density functional theory: predicting and understanding chemistry. *Rev. Comput. Chem.* **2000**, *15*, 1−86.

(11) Pinter, B.; Broeckaert, L.; Turek, J.; Růžička, A.; De Proft, F. Dimers of N-heterocyclic carbene copper, silver, and gold halides: probing metallophilic interactions through electron density based concepts. *Chem. - Eur. J.* **2014**, *20*, 734−744.

(12) Schwarz, W. H. E.; van Wezenbeek, E. M.; Baerends, E. J.; Snijders, J. G. The origin of relativistic effects of atomic orbitals. *J. Phys. B: At., Mol. Opt. Phys.* **1989**, *22*, 1515−1529.

DOI: 10.1021/acs.inorgchem.7b02994
Inorg. Chem. 2018, 57, 2603−2608